Ab initio study of thermoelectric transport properties of pure and doped quaternary compounds

C. Sevik and T. Çağın
Artie McFerrin Department of Chemical Engineering & Material Science and Engineering, Texas A&M University, College Station, Texas 77845-3122, USA

(Received 27 March 2010; revised manuscript received 1 June 2010; published 14 July 2010)

Recent experiments on thermoelectric characterization of doped quaternary compounds of sattanite or kesterite-type $Cu_2ZnSnSe_4$, Cu_2ZnSnS_4, and $Cu_2CdSnSe_4$, show promise for their use as bulk thermoelectrics. In this paper we present and discuss the energetic, electronic, and transport properties of several tetrahedrally bonded quaternary compounds Cu_2QSnX_4, where Q=Zn,Cd; X=S,Se,Te and their alloyed/doped structures, Cu doped at Q sites and M doped (M=Al,Ga,In) at Sn sites, for elucidating their thermoelectric performance. In our calculations, using density-functional theory and Boltzmann transport equations, we determine Seebeck coefficients, conductivities, power factors, a simple measure "maximum" ZT for each compound at experimentally amenable doping levels. Based on the electronic-structure and transport property calculations, we conclude that the base compounds and several doped compounds show similar potential as thermoelectric materials to the experimentally characterized one.

DOI: 10.1103/PhysRevB.82.045202 PACS number(s): 71.20.Nr, 72.20.Pa, 72.80.Jc

I. INTRODUCTION

As the worldwide concern over environmental impact and limited resources for fossil fuels intensifies, energy harvesting, and energy conversion from various sources have become very active area of research. In this context, thermoelectric materials for harvesting waste heat and converting this heat into usable electrical energy for applications such as power generation and solid-state refrigeration[1,2] is attracting increasing attention in recent years. The thermoelectric performance of a material is characterized by a dimensionless figure of merit, $ZT=S^2\sigma T/(\kappa_e+\kappa_L)$, where S is the Seebeck coefficient, σ is the electrical conductivity, T is the absolute temperature, and κ_e and κ_L are the electronic and lattice thermal conductivities of the material, respectively. Most commonly used optimized Bi_2Te_3-Sb_2Te_3 alloys have a ZT value around 1 under ambient conditions. Over the years various efficient thermoelectric materials based on clathrates,[3,4] skutterudites,[5,6] and disordered[7,8] and nanostructured[9–11] materials have been developed, and even materials with ZT values more than 2.0 have been reported.[9] However, the quest for abundant and possibly bulk thermoelectric materials with low thermal conductivity (κ) and high mobility for wide range of application is still ongoing.[8,12]

In recent experiments on quaternary tetrahedrally bonded stannite-type structures, $Cu_2ZnSnSe_4$, Cu_2ZnSnS_4, and $Cu_2CdSnSe_4$, optimized through indium doping to Sn sites and excess Copper doping as substituents at Zn and Cd sites, have been promoted as new class of wide-band-gap p-type potential thermoelectric materials. Experiments, indeed, have shown that these materials show fairly good thermoelectric performance, despite their base compounds being wide-band gap and low mobility materials.[13–15] The reported maximum ZT values are 0.37 at 700 K and 0.95 at 850 K for $Cu_2ZnSn_{1-x}In_xSe_4$, 0.45 at 700 K, 0.91 at 850 K for $Cu_{2+x}Zn_{1-x}SnSe_4$, and 0.65 at 700 K for $Cu_{2+x}Cd_{1-x}SnSe_4$. The observed surprising performance, which is very competitive with the p-type filled skutterudities at high temperatures, has been explained by the relatively low thermal conductivity, which is around 1 W/mK at 700 K for all compounds, and pretty good p-type conduction achieved with In and Cu doping. Also, the measured low thermal conductivity, which is very low, comparable to the well-known thermoelectric materials,[16,17] and its sudden decrease with temperature have been attributed to natural distorted chalcopyritelike structures of these materials and phonon-scattering centers formed especially by the Cu and In dopings. Besides, the likely coexistence of stoichiometrically similar but different crystallographic phases[18–20] have also been pointed out as another yet possible effect on low thermal conductivity.[21]

In addition to their surprising thermoelectric performance, the materials, Cu_2ZnSnS_4 and $Cu_2ZnSnSe_4$ have drawn significant interest for environmentally amenable solar-cell applications[22,23] because of their appropriate band gap around 1.5 eV (Refs. 22 and 24–27) and high optical-absorption property. This remarkable multifunctionality makes these potential thermoelectric materials a good candidate for new-generation energy harvesting materials in such applications as photothermo electrics.[28]

In this study, our main objective is to conduct an extensive theoretical investigation and develop a possible explanation of the favorable electronic-structure and thermoelectric transport properties of these new type potential thermoelectric materials. Thus, we have studied the first-principles thermoelectric properties of Cu_2QSnX_4, X=S, Se, and Te and Q=Zn,Cd with three different crystal structures and four different doping elements, Al, Ga, In, and Cu, using *ab initio* density-functional theory (DFT) and Botzmann transport theory.

The paper is organized as follows: in Sec. II, we describe our computational method and choices made for various parameters involved in DFT calculations. In Sec. III, we present our results and relevant discussion on the electronic-structure and transport properties of the systems studied. Finally, in the last section we summarize our findings and conclusions.

II. COMPUTATIONAL APPROACH AND METHODS

First-principles calculations have been performed with VASP (Refs. 29–33) within the Perdew-Burke-Ernzerhof [34] form of generalized gradient approximation (GGA). For all simulations, 450 eV plane-wave energy cutoff has been used to limit the total-energy convergence to less than 5 meV. Structural properties have been calculated using an $8\times8\times8$ Monckhorst-Pack k mesh whereas the electronic properties have been obtained using $26\times26\times26$ Monckhorst-Pack k-point grid. For GGA pseudopotentials, the valence configurations of the constituent atoms have been chosen as Cu($3d^{10}4s^1$), Zn($3d^{10}4s^2$), Cd($4d^{10}5s^2$), Sn($5s^2p^2$), Al($3s^2p^1$), Ga($3d^{10}4s^2p^1$), In($4d^{10}5s^2p^1$), S($3s^2p^4$), Se($4s^2p^4$), and Te($5s^2p^4$).

Transport calculations have been performed through solving Boltzmann transport equations within the rigid band and constant relaxation-time (τ) approximations as implemented in BOLTZTRAP.[35] This method has been applied successfully to several materials such as intermetallic compounds,[36] high-T_C superconductors[37] and thermoelectrics.[21,38–42]

Bulk modulus and its pressure derivative for each material have been determined by fitting the calculated equation of state data to the third-order Vinet equation of states (EOS).[43] In the Vinet EOS, the total energy as a function of volume is given as

$$E = E_0 + \frac{4B_0V_0}{(B_0'-1.0)^2} - \frac{2V_0B_0}{(B_0'-1)^2}[5+3B_0'(x-1)-3x] \times \exp\left[-\frac{3}{2}(B_0'-1)(x-1)\right], \quad (1)$$

where E_0 is the total energy, V_0 is the equilibrium volume, B_0 is the bulk modulus at $P=0$ GPa, B_0' is the first derivative of the bulk modulus with respect to pressure, and $x=(V/V_0)^{1/3}$.

III. RESULTS AND DISCUSSIONS

A. Structural properties

Structurally, these quaternary compounds, Cu_2QSnX_4 Q=Zn, Cd and X=S,Se,Te, can be crystalline in kesterite structure with space group $I\bar{4}$ and stannite structure with space group $I\bar{4}2m$, respectively.[13–15,26,27,44] In addition to these two experimentally observed crystal structures, we considered another stannite structure with space group $P\bar{4}2m$, and therefore we systematically investigated the structural properties, including the equation of states calculations, of Cu_2ZnSnX_4 X=S, Se, and Te, and $Cu_2CdSnSe_4$ with three specified crystal structures which obey the octet rule. The overall agreement between our calculated lattice constants (a_0) and tetragonality ratios ($\eta=c/2a$) of all compounds with available experimental and theoretical results are quite good as shown in Table I. We found that the ground-state structure of Cu_2ZnSnX_4 X=S,Se,Te is kesterite structure ($I\bar{4}$) whereas that of the $Cu_2CdSnSe_4$ is stannite structure ($I\bar{4}2m$). However, the predicted total-energy differences between the ground state and the other two structures of all materials for different volumes are about few millielectron volt per atom as shown in Fig. 1. This results were also verified by our previous calculations[21] performed by local-density approximation (LDA) functionals as well as by others.[47–49] These small total-energy differences and calculated resembling x-ray data[21] indicate the possibility of these structures occurring as defects within a otherwise pure phase (possibility of coexistence[18–20]), which may cause a decrease in κ_L as T increases.

B. Electronical properties

Experimental observations indicate that the thermoelectric performance of $Cu_2ZnSnSe_4$, $Cu_2CdSnSe_4$, and Cu_2ZnSnS_4 are enhanced by Cu doping to Zn and Cd sites and In doping to Sn sites, through reducing the Fermi level of these materials by creating p-type carriers in them. Hence, clarifying the effect of different type of doping on the electronic structure is crucial for interpretation of their transport properties. Furthermore, extensive electronic-structure analysis of different crystal structures with nearly the same structural properties is also important to develop new types of multifunctional thermoelectric devices with very low thermal conductivity. With this in mind, first we calculated the electronic density of states (DOS) of $Cu_2ZnSnSe_4$ with three aforementioned crystal phases. We have obtained almost identical results, indicating limited effect of (Cu, Zn) cation ordering on the electronic properties, as shown in Fig. 2(a). In addition to experimentally studied Cu_2ZnSnS_4 and $Cu_2ZnSnSe_4$ compounds, we also considered $Cu_2ZnSnTe_4$, and we predicted almost equal total DOS, especially for p-type conduction region (valence region which is related to hole conductivity of p-type thermoelectric materials), as seen in Fig. 2(b). Note that, for a clear comparison of the features of DOS, we have set the top of the valence band to 0 for all crystal phases in Fig. 2(a) and for all chemical composition in Fig. 2(b). The apparent similarity implies that these three different compounds should give comparable thermoelectric performance.

To investigate the influence of doping, we have performed a set of calculations especially for *heavily* doped structures, $Cu_{2.5}Zn_{0.5}SnSe_4$, $Cu_{2.5}Cd_{0.5}SnSe_4$, and $Cu_2ZnSn_{0.5}M_{0.5}Se_4$, M=In,Al,Ga aiming to accentuate the role of doping on the electronic structure of these potential thermoelectric materials. These smaller dopant elements, Cu and M as compared to Zn and Sn for which they are substituted, slightly reduce the lattice parameters, a and c. As it is plotted in Figs. 3(a) and 3(b), the overall effect of Cu and M (In, Al, and Ga) doping on the p-type conduction region is almost negligible as that might just be considered for introducing a shift on the Fermi level of the considered base systems.

Stating briefly, the calculated electronic structures of all the compounds are found to be very similar both in magnitude and in qualitative features. Especially, the similarity of the DOS of doped compounds and different crystal phases show that doping and cation distribution have very small effect on the electronic properties of these materials. As the electronic-transport properties relevant to thermoelectric merit ZT are functions of electronic structure and the density of state of the material under consideration, and they are given as

TABLE I. Calculated lattice parameters, tetragonality ratio, and bulk modulus of quaternary compounds Cu_2ZnSnX_4, X=S, Se, and Te, and $Cu_2CdSnSe_4$ with three different crystalline structures. In the table, pw=present work. HSE: Heyd, Scuseria, Ernzerhof hybrid functional.

	Cu_2ZnSnX_4	$I\bar{4}2m$			$I\bar{4}$			$P\bar{4}2m$		
	a_0	η	B_0	a_0	η	B_0	a_0	η	B_0	Ref.
Se	5.770	1.000	56	5.771	1.000	56	5.770	1.000	56	GGA-pw
	5.604	0.999	73	5.601	1.000	73	5.604	1.000	72	LDA (Ref. 21)
	5.762	1.000		5.763	0.998					GGA (Ref. 45)
	5.606	0.995								Expt. (Ref. 25)
	5.689	0.996								Expt. (Ref. 46)
				5.680	1.000					Expt. (Ref. 22)
S	5.468	1.001	68	5.474	1.000	68	5.466	1.002	68	GGA-pw
	5.324	1.002	88	5.324	1.001	88	5.323	1.001	88	LDA (Ref. 21)
	5.458	1.004		5.467	0.999					GGA (Ref. 45)
	5.438	1.006		5.448	0.999		5.446	0.999		HSE (Ref. 47)
	5.436	1.001								Expt. (Ref. 27)
				5.427	1.001					Expt. (Ref. 44)
	5.449	0.9871								Expt. (Ref. 13)
Te	6.197	0.995	44	6.183	1.001	45	6.193	0.996	44	GGA-pw
	6.016	0.997	60	6.014	0.999	60	6.016	0.997	60	LDA (Ref. 21)
	$Cu_2CdSnSe_4$									
	5.922	0.980	53	5.872	1.006	53	5.914	0.985	53	GGA-pw
	5.833	0.996								Expt. (Ref. 46)

$$\sigma = e^2 \int d\epsilon \left(-\frac{\partial f_0}{\partial \epsilon} \right) \Xi(\epsilon), \tag{2}$$

$$S = \frac{ek_B}{\sigma} \int d\epsilon \left(-\frac{\partial f_0}{\partial \epsilon} \right) \Xi(\epsilon) \frac{\epsilon - \mu}{k_B T}, \tag{3}$$

$$\kappa_e = k_B^2 T \int d\epsilon \left(-\frac{\partial f_0}{\partial \epsilon} \right) \Xi(\epsilon) \left[\frac{\epsilon - \mu}{k_B T} \right]^2, \tag{4}$$

where f_0 is the Fermi distribution function, $\Xi(\epsilon)$ is the transport distribution as defined in Ref. 38, μ is the chemical potential, and k_B is the Boltzmann's constant. One needs to see the resulting thermoelectric performance characteristics directly from these transport properties. In the next section, we discuss the relevant transport properties using calculated electronic-structure and density of states data for all the compounds considered in this section.

C. Transport properties

Initially, the transport properties of experimentally studied material $Cu_2ZnSnSe_4$ with $I\bar{4}2m$ structure were calculated to shed some light on its surprising thermoelectric performance. Aiming to get an estimate of its efficiency, we have used a specific measure, so-called *"maximum"* thermoelectric figure of merit $ZT_e = S^2\sigma/\kappa_e$, in addition to conductivity over relaxation time (σ/τ) and Seebeck coefficient S (relaxation-time independent) as a function of chemical potential (Fermi level) which is fixed to 0 at the top of the valence band and represented as minus for hole-doped region and fixed the bottom of conduction band to 0 as well and represented as plus for electron-doped region. This representation is very favorable to compare transport properties of the compound having different electronic band gap. Here, in Fig. 4 we present these properties separately at three different temperatures, namely, T: 300, 500, and 800 K.

The electrical conductivity over relaxation time (σ/τ) for all temperatures, T, are around typical values of wide-band-gap semiconductor thermoelectric materials.[40,42,50] However, the calculated S values, especially within the range of reasonable chemical potentials, μ, are at least three times larger than those of similar type of thermoelectric[40] compounds. The calculated maximum thermoelectric figure of merit, ZT_e, yielding around 0.7 with increasing T at moderate doping levels, falls between the experimentally measured values 0.37 at 700 K and 0.95 at 850 K.[13]

In order to have a comparative assessment for the thermoelectric performance of $Cu_2ZnSnSe_4$, we calculated the transport properties of widely studied thermoelectric materials $SrTiO_3$ with VASP and Bi_2Te_3 but with WIEN2K program (which employs the full potential, linearized augmented plane-wave methods and local-orbital methods including spin-orbit interaction). Especially at the moderate doping levels, better performance associated with slightly higher ZT_e

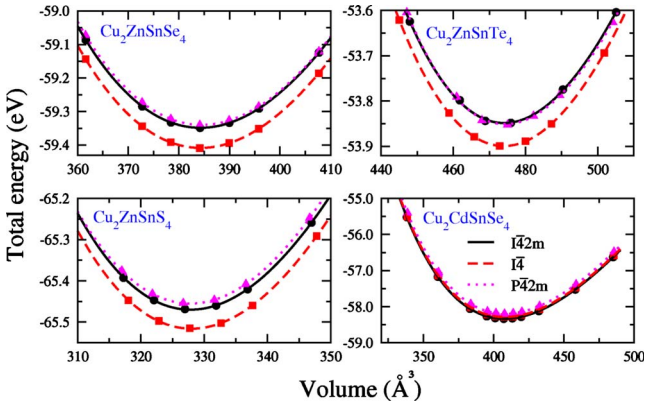

FIG. 1. (Color online) Calculated Vinet equation of states of quaternary compounds Cu_2ZnSnX_4, X=S, Se, and Te, and $Cu_2CdSnSe_4$ with three different crystalline structures. The symbols are the calculated total-energy values from DFT, the lines represent the corresponding Vinet equation of state fit to the data.

values were obtained for these quaternary compounds as shown in Fig. 5. These results corroborate that $Cu_2ZnSnSe_4$ might be as efficient as the well-known thermoelectric material Bi_2Te_3 but its maximum ZT value could not be larger than 1.

To clarify the effect of different crystal structures on thermoelectric performance, we calculated transport properties of $I\bar{4}$, $I\bar{4}2m$, and $P\bar{4}2m$ types of $Cu_2ZnSnSe_4$, Cu_2ZnSnS_4, and $Cu_2ZnSnTe_4$ crystals. Not surprisingly, calculated p-type transport properties, representing the identical σ/τ, S, and ZT_e for different type of crystal structures, are parallel with DOS results shown in Fig. 2. We obtained nearly the same structure-dependent transport properties, which provides another alternative compound to the experimentally studied ones with high electrical and low thermal conductivity, as can easily be seen in Fig. 6 displaying results for $Cu_2ZnSnSe_4$ at 500 K.

In the light of nearly identical transport properties results obtained for different crystal structures, we only compared

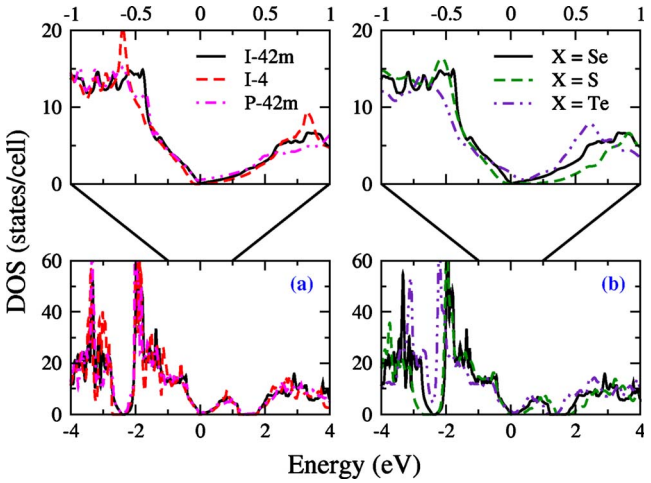

FIG. 2. (Color online) Electronic density of states of (a) $Cu_2ZnSnSe_4$ with three different crystal structures: $I\bar{4}$, $I\bar{4}2m$, and $P\bar{4}2m$, and (b) Cu_2ZnSnX_4, X=S, Se, and Te, with $I\bar{4}2m$ crystal structure. Top of the valence band is set to 0.

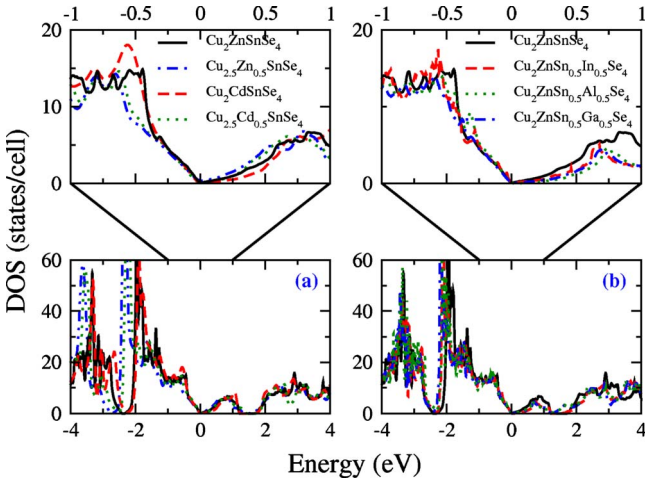

FIG. 3. (Color online) Electronic density of states of (a) $Cu_2ZnSnSe_4$, $Cu_{2.5}Zn_{0.5}SnSe_4$, $Cu_2CdSnSe_4$, and $Cu_{2.5}Cd_{0.5}SnSe_4$, (b) $Cu_2ZnSnSe_4$, and $Cu_2ZnSn_{0.5}M_{0.5}Se_4$, M=In, Al, Ga with $I\bar{4}2m$ crystal structure. Top of the valence band is set to 0.

the transport properties of the experimentally studied, $I\bar{4}2m$ phase of $Cu_2ZnSnSe_4$ and $Cu_2CdSnSe_4$ as well as their fully relaxed *heavily* Cu-doped forms, $Cu_{2.5}Zn_{0.5}SnSe_4$ and $Cu_{2.5}Cd_{0.5}SnSe_4$. The p-type transport results for the compounds containing Zn and Cd confirm the nearly identical thermoelectric performance prediction by experiment,[13–15] as seen in Fig. 7. Furthermore, similar transport coefficients of *heavily* Cu-doped forms show negligible effect of doping on p-type conduction, especially at moderate doping levels, and straighten the rigid-band shift approximation which assumes that the alloy and the pure structure have similar transport coefficients at the same carrier concentration.

In addition to Cu-doped compounds we also analyzed the transport properties of fully relaxed highly doped structures,

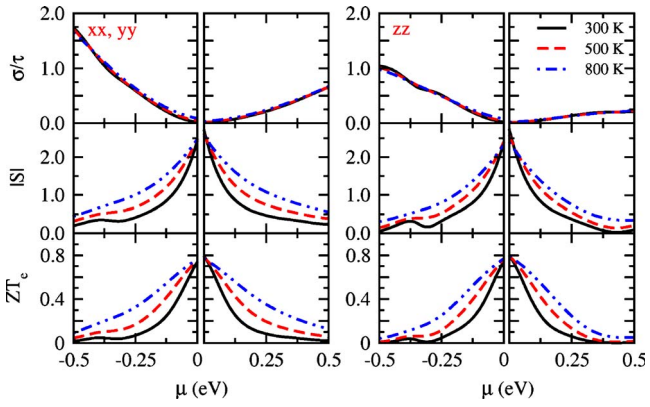

FIG. 4. (Color online) For $Cu_2ZnSnSe_4$ with $I\bar{4}2m$ crystal structure, variation in electrical conductivity over relaxation time (σ/τ), Seebeck coefficient (S), and maximum thermoelectric figure of merit ($ZT_e = S^2\sigma/\kappa_e$), as a function of chemical potential (μ). Here, σ/τ and S are in units of $10^{20}/(\Omega ms)$ and 10^2 μV/K. The solid (black), dashed (red), and dash-dot (blue) lines show data for 300 K, 500 K, and 800 K, respectively. μ is fixed to 0 at the top of the valence band and represented as minus for hole-doped region and fixed to 0 at the bottom of the conduction band and represented as plus for electron-doped region.

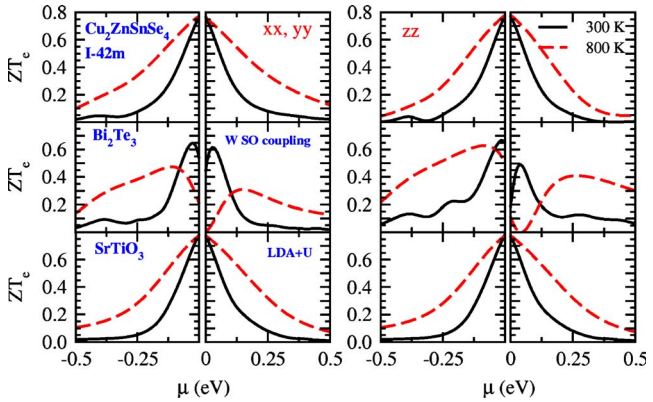

FIG. 5. (Color online) Maximum thermoelectric figure of merit ($ZT_e = S^2\sigma/\kappa_e$) of $Cu_2ZnSnSe_4$ with $I\bar{4}2m$ crystal structure, Bi_2Te_3 and $SrTiO_3$. The black straight and red dashed lines show data for 300 K and 800 K, respectively. μ is fixed to 0 at the top of the valence band and represented as minus for hole-doped region and fixed to 0 at the bottom of the conduction band and represented as plus for electron-doped region.

$Cu_2ZnSn_{0.5}M_{0.5}Se_4$, M=In, Al, Ga. In spite of excessive doping with three different IIIA group elements, the insubstantial effect of doping on *p*-type transport properties stands out once again as seen in Fig. 8. To obtain a direct comparison with experiment, we calculated the carrier concentration in terms of chemical potential for each T by using equation

$$n = \int D_e(\epsilon)\frac{1}{e^{(\mu-\epsilon)/k_BT}+1}d\epsilon, \tag{5}$$

where; n, ϵ, and D_e are the carrier concentration, energy, and first-principles DOS, respectively. Considering almost identical transport results of *heavily* doped materials shown in Figs. 7 and 8, DOS and transport data of undoped $Cu_2ZnSnSe_4$ were used to calculate the following transport properties of experimentally studied, slightly doped $Cu_2ZnSn_{1-x}In_xSe_4$ compounds. Figure 9 shows S vs T, obtained by using the calculated n, and μ relation for the four different In doping levels of $Cu_2ZnSn_{1-x}In_xSe_4$ reported by Chen[13] *et al.*

Our results for S have pretty good agreement with the experiment at x=0.05, 0.10, and 0.15 leading to similar carrier concentrations and S vs T behavior. However, for x=0, the S vs. T curve agrees at a concentration of 1×10^{20} e/cm^3, ten times higher than the experimentally re-

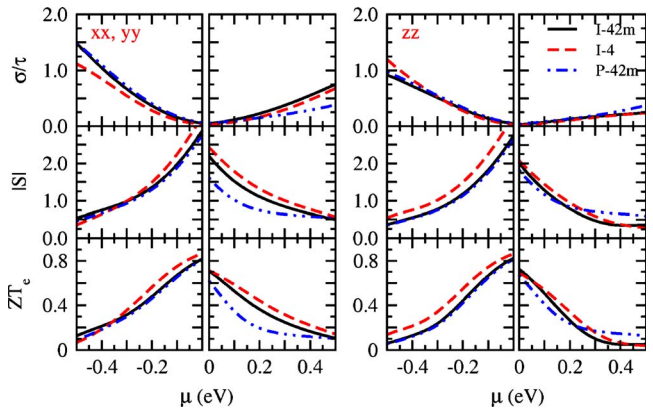

FIG. 6. (Color online) For $Cu_2ZnSnSe_4$, variation in electrical conductivity over relaxation time (σ/τ), Seebeck coefficient (S), and maximum thermoelectric figure of merit ($ZT_e = S^2\sigma/\kappa_e$), as a function of chemical potential (μ) at 800 K. Here, σ/τ and S are in units of $10^{20}/(\Omega\,\mathrm{m\,s})$ and 10^2 μV/K. The black straight, red dashed, and blue dashed-dotted lines show data for $I\bar{4}2m$, $I\bar{4}$, and $P\bar{4}2m$ crystal structures, respectively. μ is fixed to 0 at the top of the valence band and represented as minus for hole-doped region and fixed to 0 at the bottom of the conduction band and represented as plus for electron-doped region.

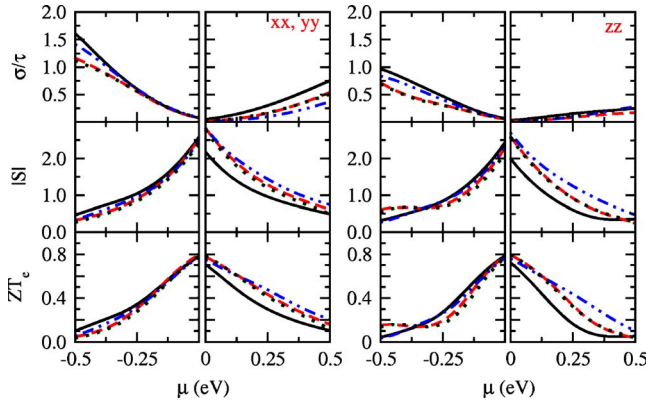

FIG. 7. (Color online) For $Cu_2ZnSnSe_4$, $Cu_{2.5}Zn_{0.5}SnSe_4$, $Cu_2CdSnSe_4$, and $Cu_{2.5}Cd_{0.5}SnSe_4$ variation in electrical conductivity over relaxation time (σ/τ), Seebeck coefficient (S), and maximum thermoelectric figure of merit ($ZT_e = S^2\sigma/\kappa_e$), as a function of chemical potential (μ) at 800 K. Here, σ/τ and S are in units of $10^{20}/(\Omega\,\mathrm{m\,s})$ and 10^2 μV/K. μ is fixed to 0 at the top of the valence band and represented as minus for hole-doped region and fixed to 0 at the bottom of the conduction band and represented as plus for electron-doped region.

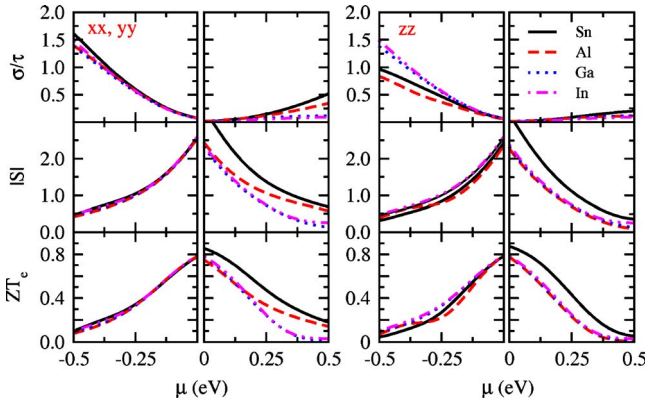

FIG. 8. (Color online) For $Cu_2ZnSn_{0.5}M_{0.5}Se_4$, M=In, Al, Ga variation in electrical conductivity over relaxation time (σ/τ), Seebeck coefficient (S), and maximum thermoelectric figure of merit ($ZT_e = S^2\sigma/\kappa_e$), as a function of chemical potential (μ) at 800 K. Here, σ/τ and S are in units of $10^{20}/(\Omega\,\mathrm{m\,s})$ and 10^2 μV/K. μ is fixed to 0 at the top of the valence band and represented as minus for hole-doped region and fixed to 0 at the bottom of the conduction band and represented as plus for electron-doped region.

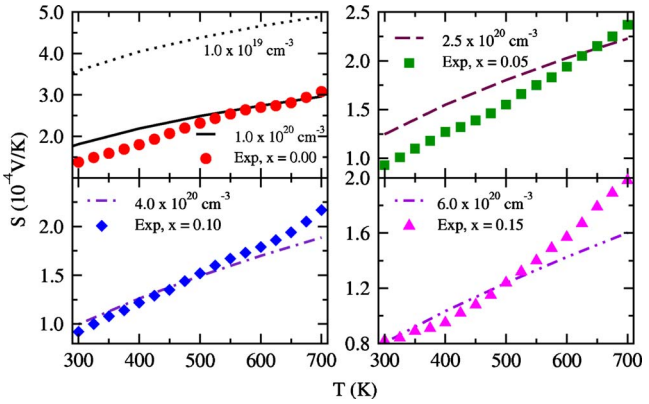

FIG. 9. (Color online) Variation in Seebeck coefficient as a function of temperature, for different carrier (In) densities, n. The data represented by dots are experimental measurements from Ref. 13.

ported hole concentration level 1×10^{19} e/cm^3. A calculation with the experimental value has the same trend but results in a 2×10^2 $\mu\mathrm{V/K}$ shift for S values. We would like to attract attention to this point in the experiment. As seen in Fig. 10 calculated σ/τ vs T increases with increase in hole concentration (In doping) as expected. To understand the overall effect of In doping, τ vs T was also calculated by fitting predicted σ/τ with σ measured by Chen[13] *et al.* and a decreasing behavior with increase in hole concentration was predicted. Furthermore, κ_e vs T has been calculated by using fitted τ; and parallel results with experiment [reported for 300 K (Ref. 13)] were obtained for all concentrations.

Particularly, to test the viability of different compounds as base materials for thermoelectric applications, we analyzed the impact of VIA group elements (S, Se, and Te) on the transport properties by considering similar band-gap values for them. As seen in Fig. 11(b) we conclude that all three materials have nearly the same potential for thermoelectric applications. Therefore, heavy doping elements reducing thermal conductivity more than light ones could be more beneficial for thermoelectric applications.

Finally, the source of low and decreasing value for κ while T increases as observed in the experiments[13] could be attributed to several factors: natural distorted structure as remarked by Chen *et al.*,[13] antiphase defects, coexistence of different polymorphs,[18–20] and possible substitutional disorder, etc. Especially the latter two might further suppress the value of κ. The likelihood of this is explored through first-principles total-energy calculations for the base structures. In addition to $I\bar{4}$, $I\bar{4}2m$, and $P\bar{4}2m$ structures, we have systematically generated several lower-symmetry structures through shuffling elements and sites with this idea in mind.[21] The energy differences between higher-energy forms $I\bar{4}2m$ and $P\bar{4}2m$ are 3.75 and 4.25 meV/atom of $I\bar{4}$ and only 0.50 meV/atom from each other. Except one $P2$ and $P\bar{4}21m$ symmetry structures, all others reported earlier by us[21] are within 15 meV/atom of $I\bar{4}$. We have also performed a representative calculation with an extended system $(2\times2\times1)$ with one antisite defect (though this represents a very large antisite defect concentration) and the energy difference per atom has been obtained as 20 meV from the defect-free cell. The small energy differences here indicate the possibility of occurrence of these structures as defects within an otherwise pure phase. Moreover, the increased probability of cation exchange structures may further decrease κ at higher T. With these observations, one might suggest several compounds with polycrystalline bulk structures with enhanced ZT or as in Bi_2Te_3/Sb_2Te_3 nanostructured/strained superlattices[51,52] constructed from similar structural/electronic properties with different chemical constitution in addition to doping of these base structures.

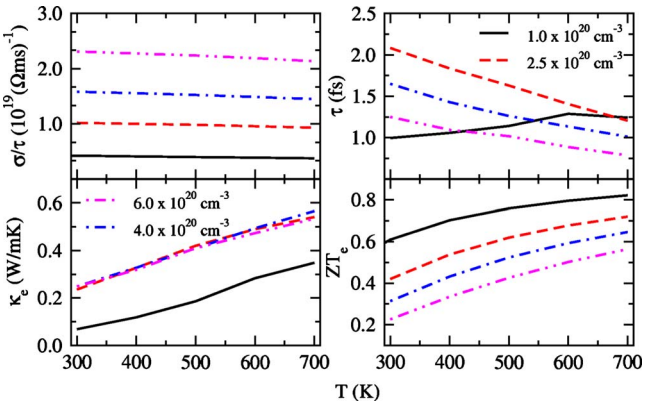

FIG. 10. (Color online) Variation in σ/τ, κ_e, τ, and ZT_e as a function of temperature, for different carrier (In) densities, n.

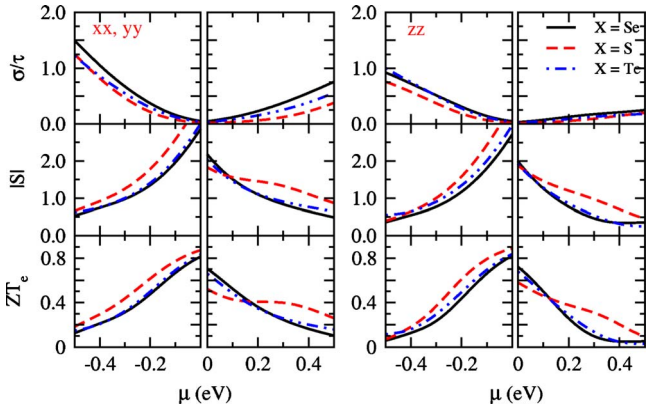

FIG. 11. (Color online) For Cu_2ZnSnX_4, variation in electrical conductivity over relaxation time (σ/τ), Seebeck coefficient (S), and maximum thermoelectric figure of merit $(ZT_e=S^2\sigma/\kappa_e)$, as a function of chemical potential (μ) at 800 K. Here, σ/τ and S are in units of $10^{20}/(\Omega\,\mathrm{m\,s})$ and 10^2 $\mu\mathrm{V/K}$. The black straight, red dashed, and blue dashed-dotted lines show data for X=Se, S, and Te, respectively. μ is fixed to 0 at the top of the valence band and represented as minus for hole-doped region and fixed to 0 at the bottom of the conduction band and represented as plus for electron-doped region.

IV. SUMMARY AND CONCLUDING REMARKS

In this paper, we presented and discussed the energetic, electronic, and transport properties of several tetrahedrally bonded quaternary compounds Cu_2QSnX_4, where Q

=Zn,Cd; X=S,Se,Te, and their alloyed structures, doped structures: Cu dopants at Q sites, (Al,Ga,In) dopants at the Sn sites, for elucidating their thermoelectric performance. From calculations, similar behavior for the electronic and transport properties has been obtained as a function of temperature, doping level, and crystal symmetry for all three. Nearly identical thermoelectric properties emerged for the different phases of each compounds. The *ab initio* total-energy calculations on different high-symmetry and other lower-symmetry structures constructed by systematically shuffling the elements and sites indicate possible sources for experimentally observed low thermal conductivity as well as attenuation with increasing temperature.

[1] F. J. DiSalvo, Science **285**, 703 (1999).
[2] G. Chen, M. S. Dresselhaus, G. Dresselhaus, J. P. Fleurial, and T. Caillat, Int. Mater. Rev. **48**, 45 (2003).
[3] C. S. Nolas, J. L. Cohn, G. A. Slack, and S. B. Schujman, Appl. Phys. Lett. **73**, 178 (1998).
[4] A. Bentien, M. Christensen, J. D. Bryan, A. Sanchez, S. Paschen, F. Steglich, G. D. Stucky, and B. B. Iversen, Phys. Rev. B **69**, 045107 (2004).
[5] B. C. Sales, D. Mandrus, and R. K. Williams, Science **272**, 1325 (1996).
[6] G. S. Nolas, D. T. Morelli, and T. M. Tritt, Annu. Rev. Mater. Sci. **29**, 89 (1999).
[7] G. J. Snyder, M. Christensen, E. Nishibori, T. Caillat, and B. B. Iversen, Nature Mater. **3**, 458 (2004).
[8] V. Ovsyannikov, V. V. Shchennikov, G. V. Vorontsov, A. Y. Manakov, A. Y. Likhacheva, and V. A. Kulbachinskii, J. Appl. Phys. **104**, 053713 (2008).
[9] R. Venkatasubramanian, E. Siivola, T. Colpitts, and B. O'Quinn, Nature (London) **413**, 597 (2001).
[10] T. C. Harman, P. J. Taylor, M. P. Walsh, and B. E. LaForge, Science **297**, 2229 (2002).
[11] H. Ohta *et al.*, Nature Mater. **6**, 129 (2007).
[12] S. V. Ovsyannikov and V. V. Shchennikov, Chem. Mater. **22**, 635 (2010).
[13] X. Y. Shi, F. Q. Huang, M. L. Liu, and L. D. Chen, Appl. Phys. Lett. **94**, 122103 (2009).
[14] M. L. Liu, F. Q. Huang, L. D. Chen, and I. W. Chen, Appl. Phys. Lett. **94**, 202103 (2009).
[15] M. L. Liu, I. W. Chen, F. Q. Huang, and L. D. Chen, Adv. Mater. **21**, 3808 (2009).
[16] G. S. Nolas, J. Sharp, and H. J. Goldsmid, *Thermoelectrics: Basic Principles and New Materials Developments* (Springer, New York, 2001).
[17] Y. Gelbstein, Z. Dashevsky, and M. P. Dariel, Physica B **391**, 256 (2007).
[18] S. Schorr, H. J. Hoebler, and M. Tovar, Eur. J. Mineral. **19**, 65 (2007).
[19] S. Schorr, Thin Solid Films **515**, 5985 (2007).
[20] D. S. Su and S. H. Wei, Appl. Phys. Lett. **74**, 2483 (1999).
[21] C. Sevik and T. Çağın, Appl. Phys. Lett. **95**, 112105 (2009).
[22] G. S. Babu, Y. B. K. Kumar, P. U. Bhaskar, and V. S. Raja, Semicond. Sci. Technol. **23**, 085023 (2008).
[23] E. Mellikov, D. Meissner, T. Varema, M. Altosaar, M. Kauk, O. Volobujeva, J. Raudoja, K. Timmo, and M. Danilson, Sol. Energy Mater. Sol. Cells **93**, 65 (2009).
[24] R. Adhi Wibowo, E. Soo Lee, B. Munir, and K. Ho Kim, Phys. Status Solidi A **204**, 3373 (2007).
[25] H. Matsushita, T. Maeda, A. Katsui, and T. Takizawa, J. Cryst. Growth **208**, 416 (2000).
[26] N. Kamoun H. bouzouita, and B. rezig, Thin Solid Films **515**, 5949 (2007).
[27] J. Zhang, L. Shoa, Y. Fu, and E. Xie, Rare Metals **25**, 315 (2006).
[28] D. Kraemer L. hu, A. Muto, X. Chen, G. Chen, and M. Chiesa, Appl. Phys. Lett. **92**, 243503 (2008).
[29] G. Kresse and J. Hafner, Phys. Rev. B **47**, 558 (1993).
[30] G. Kresse and J. Furthmüller, Phys. Rev. B **54**, 11169 (1996).
[31] R. M. Martin, *Electronic Structure* (Cambridge University Press, Cambridge, England, 2004).
[32] P. E. Blöchl, Phys. Rev. B **50**, 17953 (1994).
[33] G. Kresse and D. Joubert, Phys. Rev. B **59**, 1758 (1999).
[34] J. P. Perdew, K. Burke, and M. Ernzerhof, Phys. Rev. Lett. **77**, 3865 (1996).
[35] G. K. H. Madsen and D. J. Singh, Comput. Phys. Commun. **175**, 67 (2006).
[36] P. B. Allen and W. W. Schulz, Phys. Rev. B **47**, 14434 (1993).
[37] P. B. Allen, W. E. Pickett, and H. Krakauer, Phys. Rev. B **37**, 7482 (1988).
[38] T. J. Scheidemantel, C. Ambrosch-Draxl, T. Thonhauser, J. V. Badding, and J. O. Sofo, Phys. Rev. B **68**, 125210 (2003).
[39] G. K. H. Madsen, J. Am. Chem. Soc. **128**, 12140 (2006).
[40] J. Yang, H. Li, T. Wu, W. Zhang, L. Chen, and J. Yang, Adv. Funct. Mater. **18**, 2880 (2008).
[41] B. L. Huang and M. Kaviany, Phys. Rev. B **77**, 125209 (2008).
[42] A. Kınacı, C. Sevik, and T. Çağın (unpublished).
[43] P. Vinet, J. Ferrante, J. H. Rose, and J. R. Smith, J. Geophys. Res. **92**, 9319 (1987).
[44] S. R. Hall, J. T. Szymański, and J. M. Stewart, Can. Mineral. **16**, 131 (1978).
[45] S. Chen, G. X. Gong, A. Walsh, and S.-H. Wei, Appl. Phys. Lett. **94**, 041903 (2009).
[46] I. D. Olekseyuk, L. D. Gulay, I. V. Dydchak, L. V. Piskach, O. V. Parasyuk, and O. V. Marchuk, J. Alloys Compd. **340**, 141 (2002).
[47] J. Paier, R. Asahi, A. Nagoya, and G. Kresse, Phys. Rev. B **79**, 115126 (2009).
[48] A. Nagoya, R. Asahi, R. Wahl, and G. Kresse, Phys. Rev. B **81**, 113202 (2010).
[49] S. Chen, X. G. Gong, A. Walsh, and S. H. Wei, Phys. Rev. B **79**, 165211 (2009).
[50] S. Ohta, T. Nomura, H. Ohta, and K. Koumoto, J. Appl. Phys. **97**, 034106 (2005).
[51] G. Wang and T. Çağın, Appl. Phys. Lett. **89**, 152101 (2006).
[52] G. Wang and T. Çağın, Phys. Rev. B **76**, 075201 (2007).